Edge Localised Modes in Tokamak Plasmas

github.com/tobiasschuett/ELMs

Tobias Schuett - tms535@york.ac.uk

UNIVERSITY of York

1. Introduction

- Tokamak fusion reactors are a promising way to achieve commercially available fusion energy by creating an ionised gas called plasma
- After a certain plasma heating power is reached, the tokamak plasma can transition to the high confinement regime (H-mode) with higher core plasma densities and temperatures
- Once in H-mode, the magnetically confined plasma shown in fig. 1 develops quasi-periodic instabilities that are called edge localised modes (ELMs) which lead to particle transport out of the core plasma
- These modes are problematic for future reactors such as ITER due to their high heat flux on plasma facing components (PFC) that can lead to a less stable plasma due to higher impurity densities
- Gas puff imaging (GPI) and the outer divertor current (Ipolsola) are two diagnostics in the ASDEX Upgrade tokamak (AUG) that are used in this report to detect the ELMs and to analyse their characteristics
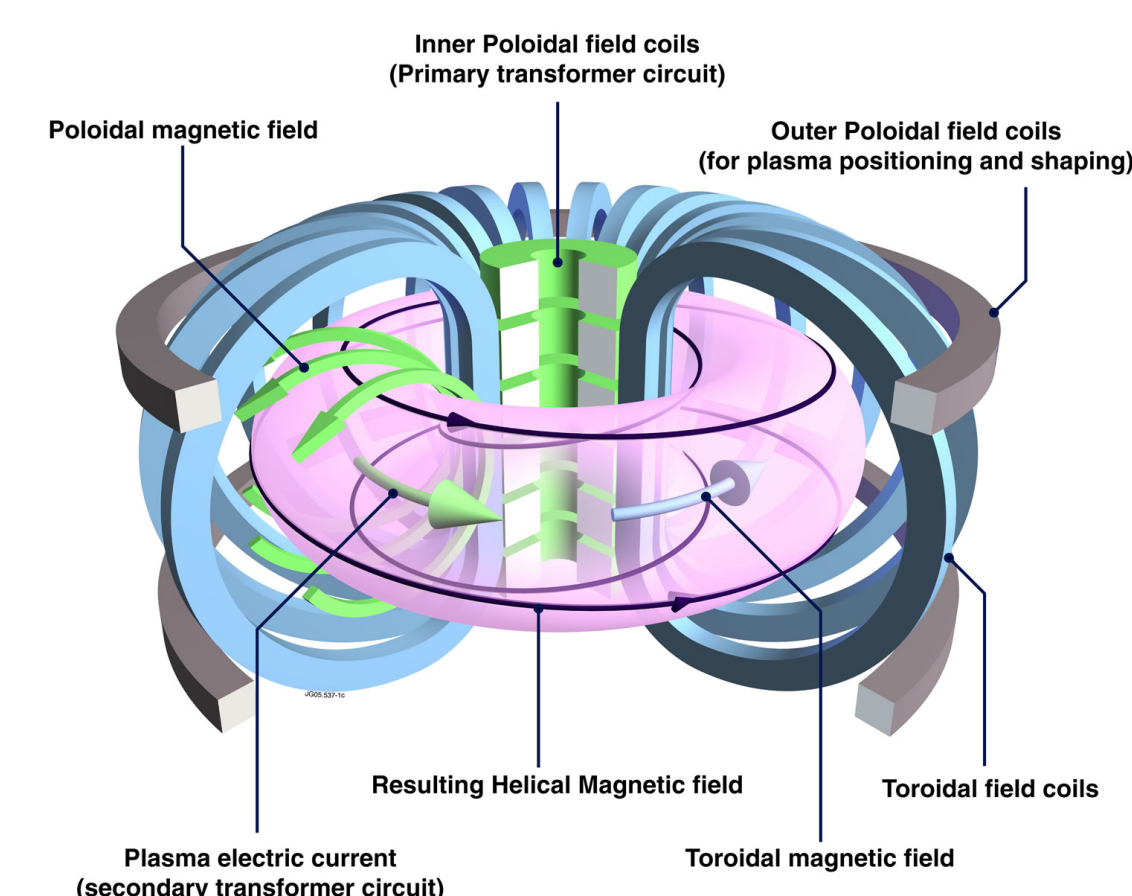

Fig. 1: The tokamak working principles. Taken from [1].

2. Methods

Fig. 2: Diagnostics in AUG

- GPI uses neutral gas injection at the edge of the core plasma to measure the plasma density ...
- Ipolsola ... measures ... tokamak ...
- ... frequency in power spectrum
- ELM detection mechanism ... forward difference of ... currents (intensity change ...) (GPI)
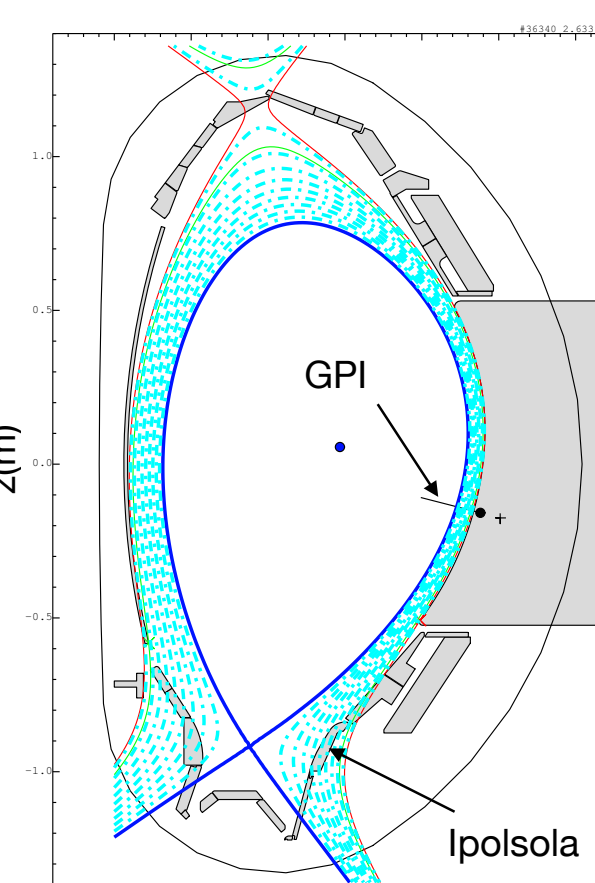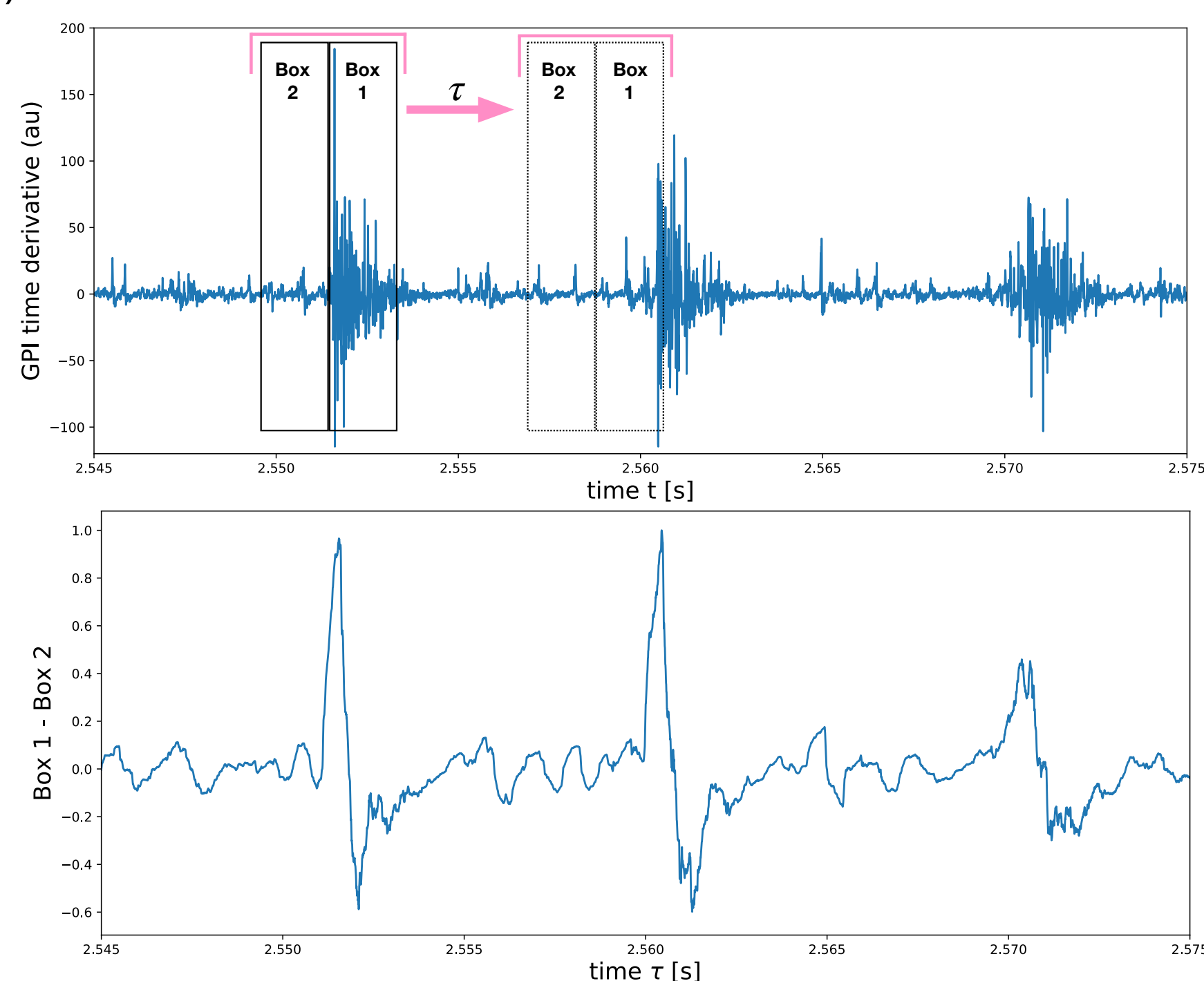

Fig. 3: M1 working principles

- Mechanism 2 uses the cross-correlation of a single ELM s and the full signal g as shown in fig. 4. The cross-correlation shows local maxima for shift times τ where s and g are similar in shape
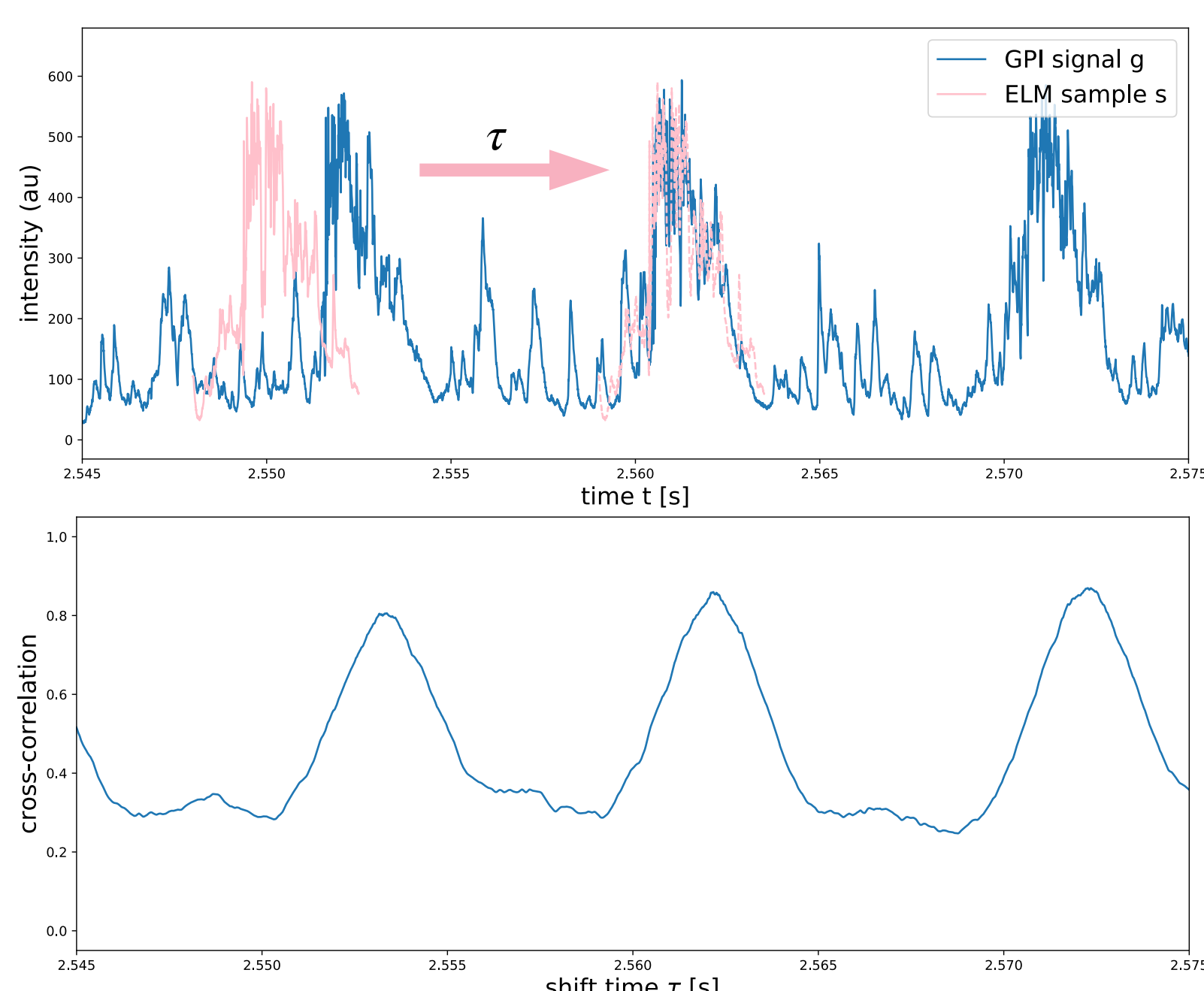

Fig. 4: M2 working principles

Detection Idea: local peaks in figure 3 and 4 correspond to ELM

- Both mechanisms have 2 input parameters:
  - *flagging threshold* (tres): minimum peak height required
  - *flagging delta* (flagd): minimum distance between two ELMs

- M1 and M2 were combined into mechanism CM. CM takes as input the flags generated by M1 and M2, and outputs a list of flags each with an additional attribute indicating whether this flag was raised by both/M1-only/M2-only

Acknowledgement

I would like to thank Dr. István Cziegler for supervising my work for this thesis and for providing guidance along the way. Special thanks to Steven Thomas for contributing to the work done on the Ipolsola and GPI offset, for providing figure 2 for this thesis and for giving me access to additional experimental data whenever needed.

3. Results

3.1 Mechanism Performance

- Optimal parameter pair determined by creating a time series where the ELMs are labelled and minimising loss L in parameter space:

$$L(\text{thres, flagd}) = fp(\text{thres, flagd}) + fn(\text{thres, flagd})$$

- CM generally adopts the higher false positive rate and lower false negative rate of either M1 and M2. This minimises falsely included data for characteristics analysis in 3.3
- When removing ELMs from data, it is more useful to accept any detection by M1/M2/CM

#36341 - GPI	Mechanism 1	Mechansims 2	Combi Mechanism
fp(thres,fdelta) [%]	11.69	4	2.38
fn(thres,fdelta) [%]	9.52	17.14	23.81
L(thres,fdelta) [%]	**21.21**	**21.14**	**26.19**

#36341 - Ipolsola	Mechanism 1	Mechansims 2	Combi Mechanism
fp(thres,fdelta) [%]	4.17	3.23	3.45
fn(thres,fdelta) [%]	2.86	8.57	11.43
L(thres,fdelta) [%]	**7.03**	**11.8**	**14.88**

Table 1: The loss values in GPI and Ipolsola of M1/M2/CM.

3.2 Ipolsola and GPI offset

- ELM triggers sound wave disturbance that follow the magnetic field lines once entering the scrape-off layer shown in light blue dotted lines in fig. 2
- Median offset between flags in Ipolsola and GPI measured to be $\Delta t = (2.17 \pm 0.15)\,\text{ms}$
- Calculations based on ion sound speed and distance between GPI and Ipolsola suggest an expected offset of $\sim 18\,\mu s$
- The works of Manfredi *et al.* suggest an offset of a few hundred microseconds
- This offset is not of physical origin, but caused by a mismatch in the involved clocks
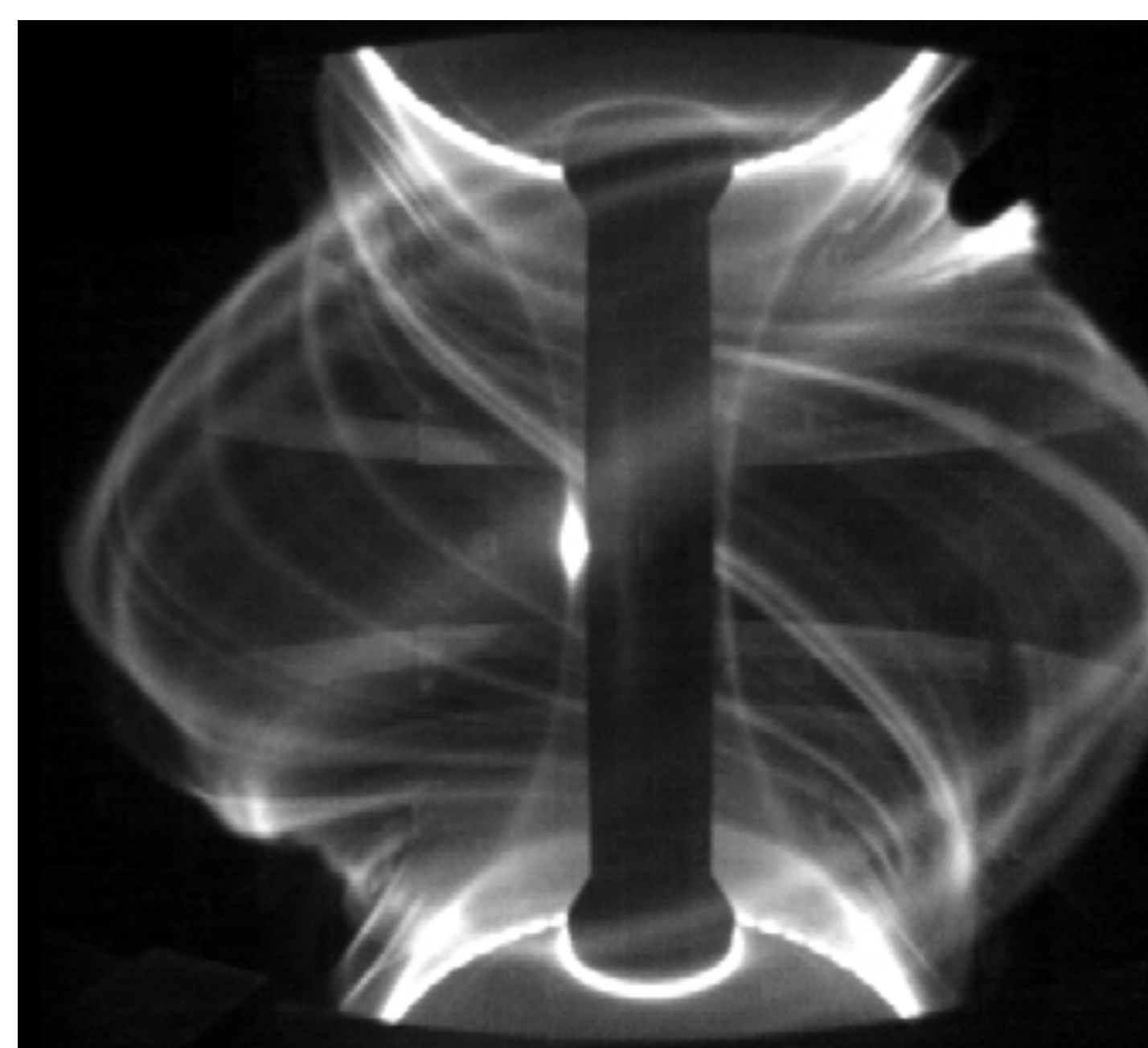
How to detect this → in here

Fig. 5: ELM picture in MAST. Taken from [2].
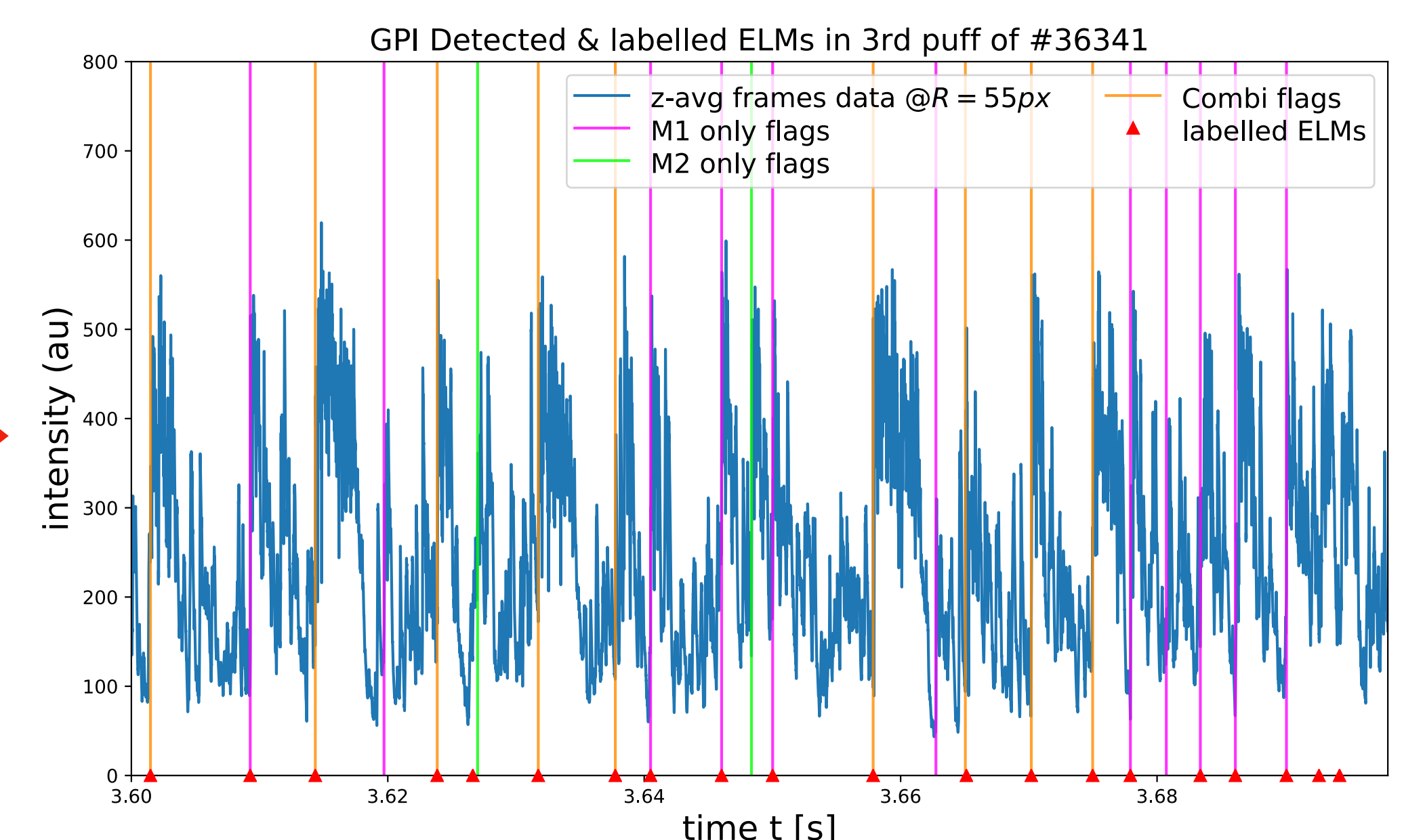

Fig. 6: Detected ELMs by CM/M1/M2 against the labelled ELMs in the GPI data.

3.3 Temporal Shape

- 230 (210) ELMs were detected by CM in the GPI (Ipolsola)
- The power normalised mean ELM was obtained by averaging the signal at each point in time across all detected ELMs each of length Δt and by scaling the signal at each point in time by the reciprocal of the total ELM power:

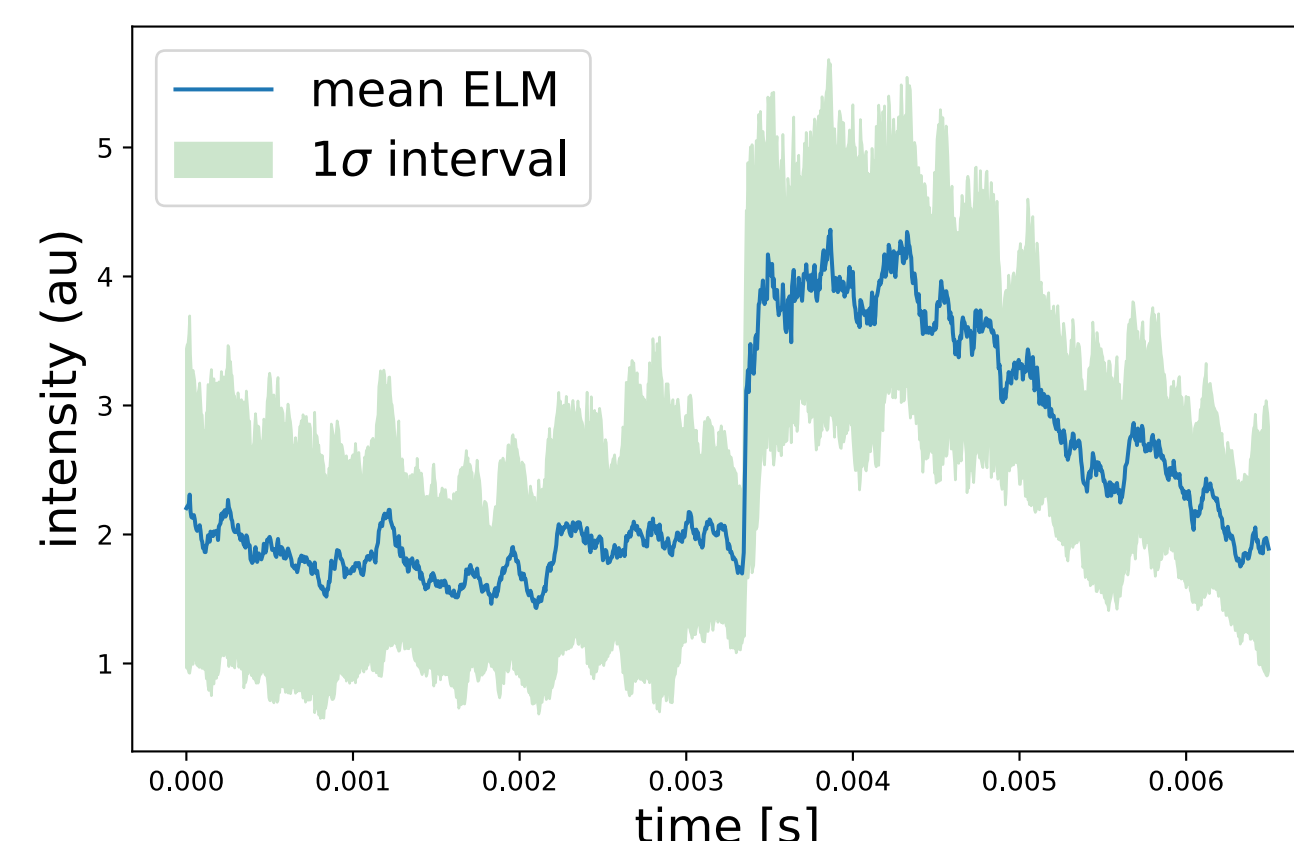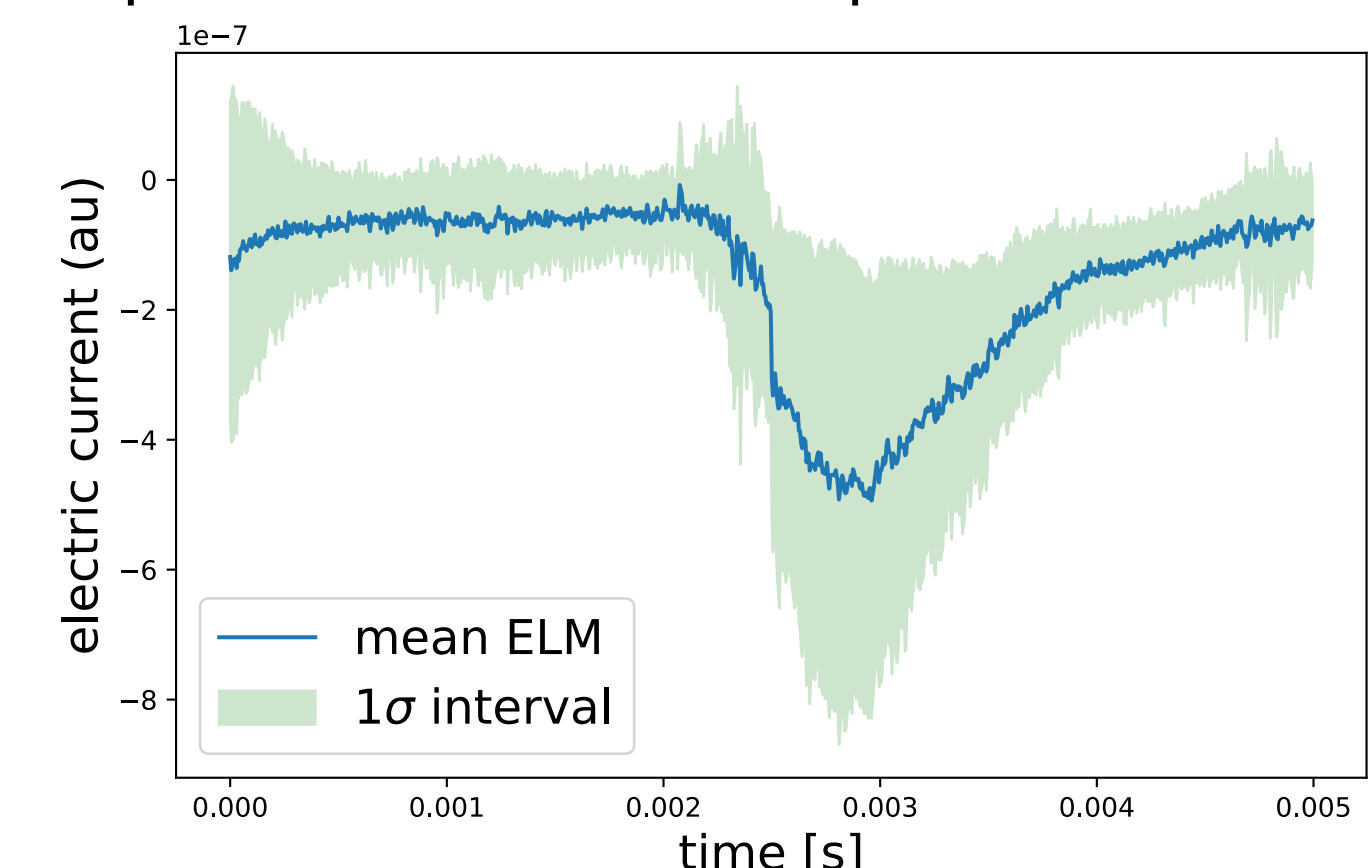**Fig. 7:** mean ELM shape in GPI data.

Fig. 8: mean ELM shape in Ipolsola data.

3.4 ELM frequency and Periodicity

- ELM period calculated as the mean time that passes between all detected ELMs
- Mean coefficient of variation (CV) is given by $36\,\%$ in the GPI and $29\,\%$ in the Ipolsola
- Perfectly periodic behavior would result in a CV value of zero
- Aperiodic behavior, i.e. a uniform distribution of T_{ELM}, would result in CV of 58%
- This confirms the quasi-periodic ELM behaviour stated in the works of Connor [4] and Keilhacker *et al.* [5]
- ELM period based on peak in power spectrum shows to be a good first approximation as it lies within the standard deviation of the ELM period in 5/7 cases (fig. 9)
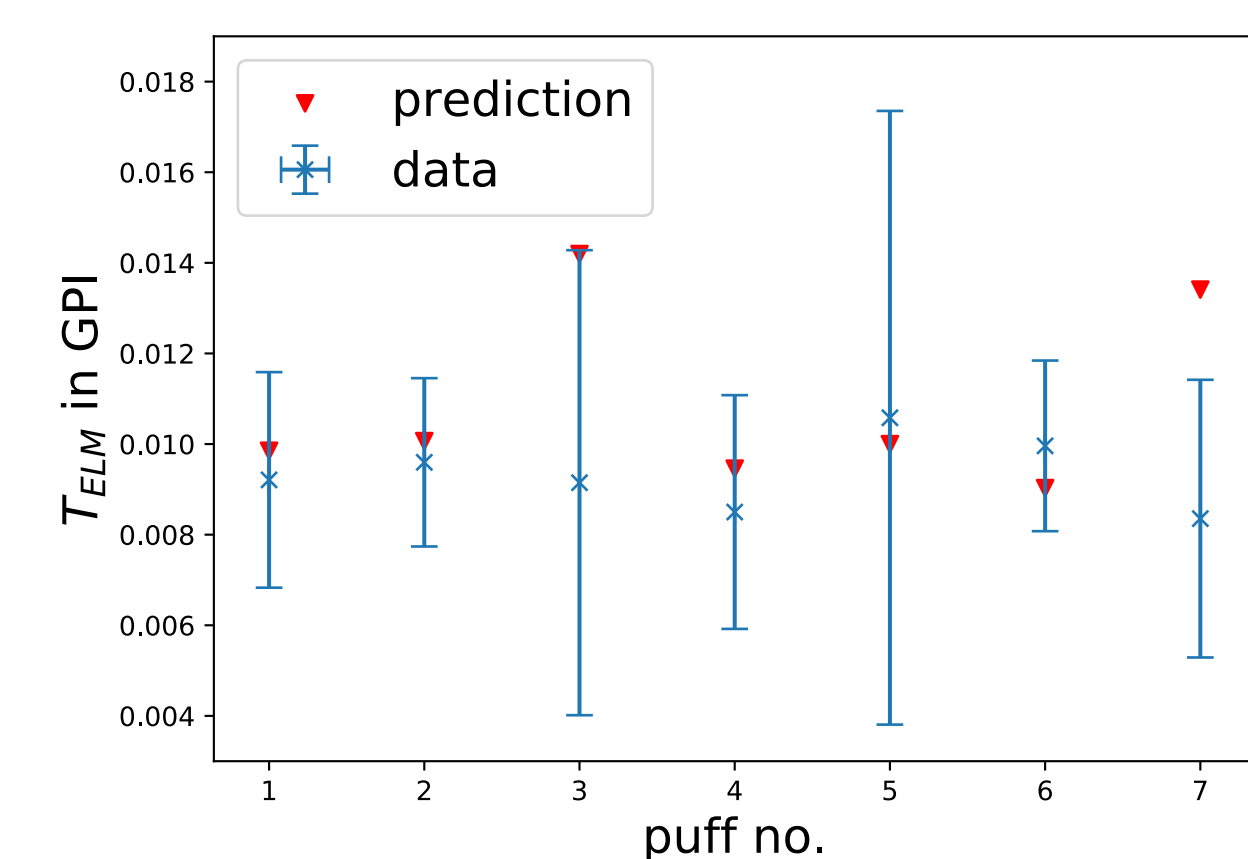

Fig. 9: mean ELM period (blue) and predicted ELM period based on peak in power spectrum of the signal (red).

4. Conclusion

- ELM detection mechanism CM developed which shows $\sim 3\,\%$ false positive rate in GPI and $\sim 4\,\%$ in Ipolsola
- Investigated time delay between ELMs in GPI and Ipolsola of $(2.17 \pm 0.15)\,\text{ms}$ shows not to be of physical origin but caused by mismatch in involved clocks
- Power normalised mean ELM averaged over 230 (210) ELMs in GPI (Ipolsola) shows more sudden increase in intensity in GPI of order of microseconds but longer increase in Ipolsola of $\sim 0.5\,\text{ms}$
- Frequency peak in power spectrum of the signal shows to be a good approximation of the ELM period in some cases
- Coefficient of variation of measured T_{ELM} of $36\,\%$ in GPI and $29\,\%$ in Ipolsola confirms quasi-periodicity of ELMs described in the works of Connor [4] and Keilhacker *et al.* [5]

References

[1] R. Pitts, R. Buttery, and S. Pinches, "Fusion: The way ahead" Phys. World, vol. 19, p. 20, 2006.
[2] A. Kirk et al. 2007 Plasma Phys. Control. Fusion **49** 1259
[3] Manfredi, G., Hirstoaga, S. & Devaux, S. Vlasov modelling of parallel transport in a tokamak scrape-off layer. *Plasma Physics and Controlled Fusion* **53,** 015012 (Nov. 2010)
[4] Connor, J. W. Edge-localized modes - physics and theory. *Plasma Physics and Controlled Fusion* **40,** 531–542 (May 1998)
[5] Keilhacker, M. *et al.* Confinement studies in L and H-type Asdex discharges. *Plasma Physics and Controlled Fusion* **26,** 49–63. (Jan. 1984)